Concepts for Sensor Matching in Mechatronic Systems

Clarence W. DE SILVA

(*Department of Mechanical Engineering*, *The University of British Columbia, Vancouver, BC V6T 1Z4*)

Abstract: A typical mechatronic system consists of a multitude of components, and the sensors belong to an important and crucial class of such components. Optimal matching of the system components is implicit in the current definition of a mechatronic system. The focus of the present paper is the optimal matching of sensors with other hardware in the system. Sensor matching may be based on several concepts such as the operating frequency range (operating bandwidth), speed of response (and the corresponding rate of data sampling in digital conversion), the device sensitivity (or gain or data amplification), and the effect of component accuracy on the overall accuracy of the system. The present paper explores all these concepts and presents suitable approaches for sensor matching through those criteria. The relevant procedures are illustrated using case studies.

Key words: Mechatronic Systems, Optimal Instrumentation, Sensor Selection, Sensor Matching

1　Introduction

The current definition [1] of a mechatronic system enhances the previously established definition, to include, multi-domain or multi-physics instead of just electromechanical products, an integrated (meaning the concurrent or simultaneous consideration various domains in the system) and unified (meaning the use of similar or analogous approaches for various domains in the system)　approach for the system development and operation rather than just an integrated approach, and a systematic approach for the system development, with a clear set of steps, leading to a "unique" outcome through design optimization. It is clear that design optimization, and hence "optimal instrumentation" is a requirement for a mechatronic system. From this enhanced definition it can be verified that a mechatronic system approach can lead to at least the following key benefits:

- Optimality and better component matching
- Increased efficiency
- Cost effectiveness
- Ease of system integration and expansion/enhancement
- Compatibility and ease of cooperation with other systems
- Improved controllability
- Increased reliability
- Increased product life

In facilitating such benefits, proper matching of sensors with the other hardware such as that for signal conditioning and amplification and for data acquisition and sampling, is important for a mechatronic system. This is the focus of the present paper.

The topic of sensor selection has been considered in other studies as well[2]. When matching a sensor with other hardware in a system, it is required to first identify the relevant matching criterion. The frequency range of operation (or, the operating bandwidth) is one

such criterion. Related to this is the speed of operation and also the rate of data sampling into a digital system (e.g., computer). The device sensitivity (or gain or data amplification) is another important criterion, which depends on the sensitivity of the individual components, including the sensor. The effect of the component accuracy, including that of the sensor, on the overall accuracy of the system is also an important criterion. The present paper considers all these criteria of sensor matching. The underlying procedures are presented and illustrated using case studies.

2 Bandwidth Considerations

Modeling considerations are important in the present context [3-5]. Also, the type of sensor and the nature of the mechatronic application are important [6]. Bandwidth has different meanings depending on the particular context and application [7, 8]. For example, when studying the response of a device, the bandwidth relates to the fundamental resonant frequency and correspondingly to the *speed of response* of the device for a given excitation. In band-pass filters, the bandwidth refers to the frequency band (*pass band*) of the signal components that are allowed through the filter, while the frequency components outside the band are rejected. With respect to measuring instruments such as sensor systems, bandwidth refers to the range frequencies within which the instrument measures a signal accurately (*operating frequency range*). As a particular note, if a signal passes through a band-pass filter we know that its frequency content is within the bandwidth of the filter, but we cannot determine the actual frequency content of the signal on the basis of that observation. In this context, the bandwidth appears to represent a *frequency uncertainty* in the observation (i.e., the larger the bandwidth of the filter, less certain is our knowledge about the actual frequency content of a signal that passes through the filter). In digital communication networks (e.g., the Internet), the bandwidth denotes the capacity (*information capacity*) of the network in terms of information rate (bits/s).

Bandwidth is an important consideration in the component matching of a mechatronic system. In this context, bandwidth concerns the frequency range of operation and also the speed of response of a device. Specifically, consider a sensor having the primary time constant τ_s. Then, it is known that its operating frequency is limited to at most $\dfrac{1}{\tau_s}$, which represents its bandwidth. Next consider a piece of analog hardware such as a filer or an amplifier having the bandwidth ω_{bw}. Then, in order to optimize the operating range of frequencies of the combined, the required matching relation is

$$\frac{1}{\tau_s} = \omega_{bw} \qquad (1)$$

Furthermore, according to Shannon's sampling theorem, the data from the combined device has to be sampled at least twice this frequency (i.e., $2\omega_{bw}$) in order to reduce the aliasing error in the sampled data.

The bandwidth of the hardware component, in the present context may mean such frequencies as the half-power bandwidth, corner frequency, or break frequency. The half-power bandwidth refers to the frequency at which the power of the component reduces to half the value (or, the signal value reduction by the factor $\sqrt{2}$). The corner frequency or the break frequency is the frequency at which the magnitude asymptote of the Bode diagram of the component changes its slope (which is at a location of a pole or zero of the transfer function). For a low-pass filter, this may also represent its roll-down frequency. For a first order device, all these quantities are equal, but this is not the case in general.

Consider the analog circuit that is connected to an analog sensor, as shown in Fig. 1. Here,

v_s = input voltage to the circuit (output of the sensor)

v_o = output voltage of the circuit.

Suppose that the time constant of the analog sensor is τ_s. In order to ideally match the sensor to the given analog circuit, we will determine the necessary relation between τ_s and the circuit parameters.

For computations, we will use the numerical values $\tau_s = 2.0$ ms, $R = 1.0$ kΩ, and $R_i = 10.0$ kΩ.

Also, we will estimate a suitable sampling frequency for the data (output) from the analog circuit into a digital device.

To obtain the circuit equation, in the time domain, we use the two properties of an op-amp: 1. Current into the op-am from each input lead is zero; 2. The potentials at the two input leads of the op-amp are equal.

From the circuit it is clear that the voltage at both the +ve lead and the –ve lead of the op-amp is v_o.

Fig. 1 identifies the nodes A and B.

First, we write the current balance equations at Node A, where the voltage is defined as v_A:

$$\frac{v_s - v_A}{R} + \frac{v_o - v_A}{R_i} + C_f \frac{d}{dt}(v_o - v_A) = 0$$

$$\rightarrow v_s - \left(1 + \frac{R}{R_i}\right)v_A + \frac{R}{R_i}v_o + RC_f \frac{dv_o}{dt} - RC_f \frac{dv_A}{dt} = 0$$

Or, $\quad v_s - (1+k)v_A + kv_o + \tau_f \frac{dv_o}{dt} - \tau_f \frac{dv_A}{dt} = 0$ (2)

where we have defined,

$$k = \frac{R}{R_i} \tag{3}$$

$$\tau_f = RC_f \tag{4}$$

Next, we write the current balance equations at Node B.

Note: The current through the +ve lead of the

op-amp is zero (a property of an op-amp). Also, the potential at Node B is v_o. $\quad \frac{v_A - v_o}{R_i} = C_i \frac{dv_o}{dt} \rightarrow$

$$v_A = v_o + R_i C_i \frac{dv_o}{dt}$$

Or, $\quad v_A = v_o + \tau_i \frac{dv_o}{dt}$ (5)

where we have defined,

$$\tau_i = R_i C_i \tag{6}$$

Eliminate v_A by substituting Equation (5) into (2).

$$v_s - (1+k)\left(v_o + \tau_i \frac{dv_o}{dt}\right) + kv_o + \tau_f \frac{dv_o}{dt} -$$

$$\tau_f \frac{d}{dt}\left(v_o + \tau_i \frac{dv_o}{dt}\right) = 0$$

We get the input-output differential equation of the circuit:

$$v_o + (1+k)\tau_i \frac{dv_o}{dt} + \tau_f \tau_i \frac{d^2 v_o}{dt^2} = v_s \tag{7}$$

Here, k, τ_f, and τ_i are as expressed in (3), (4), and (6), respectively.

Now, introduce the Laplace variable s into the input-output differential equation (7). We get the circuit transfer function,

$$\frac{v_o}{v_s} = \frac{1}{\left[\tau_f \tau_i s^2 + (1+k)\tau_i s + 1\right]}$$
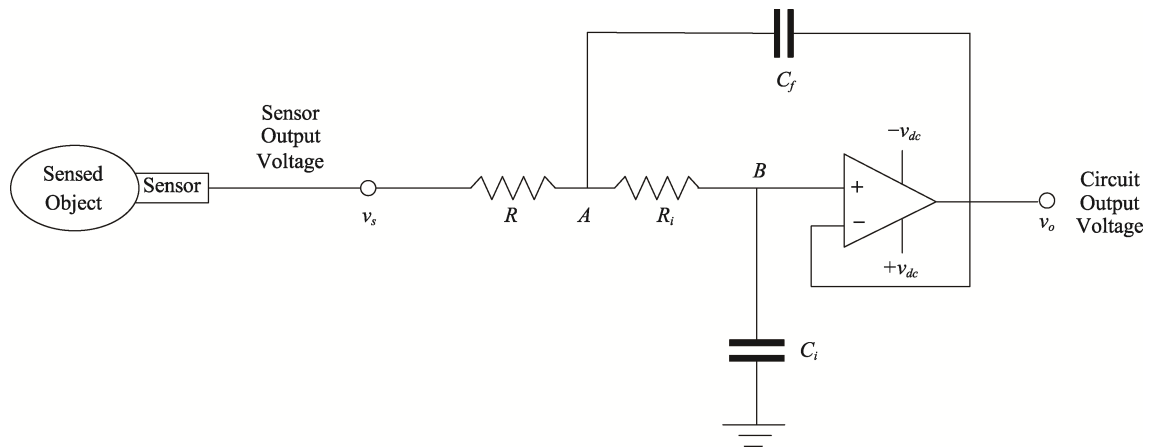
Clearly, this second-order transfer function

Fig.1   An Analog Circuit Connected to an Analog Sensor

represents a low-pass filter. It has two poles, given by the roots of the characteristic equation: $\tau_f\tau_i s^2 + (1+k)\tau_i s + 1 = 0$

The break frequency of the filter is given by the pole with the smaller magnitude. The two poles are:

$$\frac{-(1+k)\tau_i \pm \sqrt{\left[(1+k)\tau_i\right]^2 - 4\tau_f\tau_i}}{2\tau_f\tau_i}$$

The discriminant, $\left[(1+k)\tau_i\right]^2 - 4\tau_f\tau_i$, may be evaluated using (leaving out the common term τ_i),

$$(1+k)^2\tau_i - 4\tau_f = (1+\frac{R}{R_i})^2 R_i C_i - 4RC_f$$

Assume that this expression is zero. Then, the filter has two repeated poles at, $\dfrac{-(1+k)\tau_i}{2\tau_f\tau_i} = -\dfrac{(1+k)}{2\tau_f} = $

$$-\frac{\left(1+\dfrac{R}{R_i}\right)}{2RC_f}.$$

This second order filter has real poles (i.e., non-oscillatory system) not complex. Hence, it does not have a resonant frequency, and the filter bandwidth is given by the magnitude of the pole (or cut-off frequency, or break frequency or corner frequency),

$$\omega_{bf} = \frac{1}{2RC_f}\left(1+\frac{R}{R_i}\right).$$

This is not the half-power bandwidth, as verified next.

Consider the 2nd order low-pass filter with two repeated (and of course real) poles: $G(s) = \dfrac{\omega_n^2}{\left[s^2 + \omega_n^2\right]}$

Note: The transfer function is normalized, so that its magnitude at zero-frequency is 1.

From its Bode diagram it should be clear that ω_n is the break frequency or the corner frequency, which is also the roll-down frequency of the filter. Hence it can be used to represent the bandwidth of the filter. It is also the magnitude of each of the two real poles of the filter (the pole location is $-\omega_n$). However, unlike the 1st order low-pass filter, this is not the half-power

bandwidth of the filter. This can be verified as follows.

The magnitude of the transfer function is $\dfrac{\omega_n^2}{\left[\omega^2 + \omega_n^2\right]}$.

Hence, its half-power frequency is given by,

$\dfrac{\omega_n^2}{\left[\omega^2 + \omega_n^2\right]} = \dfrac{1}{\sqrt{2}}$. This evaluates to, $\omega^2 = \omega_n^2(\sqrt{2}-1)$,

or $\omega = \omega_n(\sqrt{2}-1) = 0.64\omega_n$.

This is the half-power bandwidth of the filter, which is not equal to the corner frequency (or break frequency).

The time constant of the sensor is τ_s. Hence, its half-power bandwidth is $\omega_{bs} = \dfrac{1}{\tau_s}$

Ideally, the bandwidth may be interpreted as the operating range (i.e., flat region of the transfer-function magnitude) of a filter or a sensor. Hence, for ideal matching of a sensor and a filter, we must have,

$$\omega_{bf} = \omega_{bs}$$

Accordingly, the ideal component matching (instrumentation) relationship is, $\dfrac{1}{2RC_f}\left(1+\dfrac{R}{R_i}\right) = \dfrac{1}{\tau_s}$

or,

$$\frac{\tau_s}{2RC_f}\left(1+\frac{R}{R_i}\right) = 1$$

Substitute in (8) the given numerical values:
$\tau_s = 2.0$ ms, $R = 1.0$ kΩ, $R_i = 10.0$ kΩ

$$\frac{2.0\times10^{-3}}{2\times1.0\times10^3 C_f}\left(1+\frac{1.0}{10.0}\right) = 1$$

Hence,

$$C_f = \frac{2.0\times10^{-3}}{2\times1.0\times10^3}\left(1+\frac{1.0}{10.0}\right) \text{ F} = 1.1\times10^{-6} \text{ F} = 1.1 \text{ μF}$$

The maximum bandwidth of the combined analog device is, $\omega_b = \dfrac{1}{2.0\times10^{-3}}$ rad/s = 500.0 rad/s =

$\dfrac{500.0}{2\pi}$ Hz = 79.6 Hz

According to Shannon's sampling theorem, the data sampling frequency into a digital device has to be at least twice this value ➔ >160 Hz.

3 Sensitivity Considerations

Sensitivity and sensitivity error are important rating parameters for any component in a mechatronic system. Sensitivity may be interpreted in several ways including the local slope of the input-output curve, the partial derivative of the input-output relationship, and the gain. The sensitivity of B to A indicates how B changes due to a change in A, and is expressed as

$$S_{B/A} = \frac{\Delta B}{\Delta A} \rightarrow \frac{\partial B}{\partial A} \text{ in the limit} \quad (9)$$

It is important to optimize the gain (direct sensitivity) of the overall system, and clearly this depends on the sensitivities of the individual components in the system. This aspect is investigated using a case study, which will also indicate ways to optimize the device gain.

3.1 Case Study

Consider the sensing and data acquisition arrangement shown in Figure 2. The temperature T of an object is monitored by using an RTD (resistance temperature detector). The resistance R_r of the RTD forms one branch of the Wheatstone bridge. The other three branches of the bridge have identical resistance R, which does not change due to the body temperature T. The bridge output (voltage) v_s is modified by an analog circuit. The voltage output from this circuit is sampled and digitized by an analog-to-digital converter (ADC), and read into a digital computer to process that data (for further action such as performance assessment, fault diagnosis, control).

The resistance of the RTD obeys the equation $R_r = R_{r0}(1 + \alpha \Delta T)$, where,

R_r = resistance of the RTD, in ohms (Ω), at temperature T (in °K)

R_{r0} = resistance of the RTD at temperature T_0 (the starting temperature)

$\Delta T = T - T_0$ = temperature rise (in °C)

α = temperature coefficient of RTD resistance (in /°C)

We assume that the starting temperature (the ambient temperature) T_0 is known. The corresponding RTD resistance $R_{r0} = R$ (the bridge completion resistance).

First, we will determine an equation relating the bridge output voltage v_s to the temperature change ΔT of the object (in terms of the bridge supply voltage (dc) v_{ref} and α. Next, we derive the input-output differential equation of the analog circuit (signal conversion circuit) in the figure, in terms of the circuit parameters: resistances R_a, R_b, and R_f, and capacitance C.

Circuit input voltage (sensor output) = v_s

Circuit output voltage (ADC input) = v_o

We obtain the transfer function $G(s)$ of the analog circuit from this result. We will sketch the Bode magnitude curve and the Bode phase angle curve (not to scale) of this transfer function. By examining the nature of the circuit transfer function (the analytical expression and the Bode curves), we will determine expressions for the following quantities, in terms of the circuit parameters:

(a) Steady-state gain (amplification) provided by the circuit

(b) High-frequency gain (amplification) provided by the circuit

(c) The phase "lead" angle (in radians) provided by the circuit

(d) Break points (frequencies, in radians/s) of the Bode plot.

We will indicate the benefits that this circuit provides for the overall measurement system, in different frequency ranges.

The following numerical values are given:

The maximum useful temperature change that the RTD can accurately measure (the full-scale temperature) is 100.0°C, $\alpha = 0.008$/°C, $v_{ref} = 10.0$ V.

The ADC has 8 bits. It generates its maximum count for its full-scale input 6.0 V.

The analog circuit parameters: $R_a = 10.0$ kΩ, $Rb = 2.0$ kΩ and $C = 2.0$μF. Using them we will determine a suitable value for the feedback resistor R_f in order to realize the best sensitivity (gain) for the overall arrangement (consisting of the sensor, Wheatstone bridge, analog circuit and the ADC).

We will determine three suitable frequency ranges

of operation for the system, and the operating conditions or requirements for each of these frequency ranges. Finally, we will determine a satisfactory sampling rate (of data into the computer from the ADC) in each frequency range of operation, and a suitable upper limit for the time constant of the RTD.

First, we apply $R_r = R_{r0}(1+\alpha\Delta T)$. Hence, the change in the RTD resistance $\Delta R = R_r - R_{r0}$ corresponding to the temperature change ΔT is,

$$\Delta R = R_{r0}\alpha\Delta T \tag{10}$$

It is given that,

$$R_{r0} = R \tag{11}$$

where, R is the resistances of the non-active branches of the Wheatstone bridge. Hence, the bridge is balanced in the beginning, and the bridge output is zero.

From the standard result of a Wheatstone bridge (up to the O(1) term of the Taylor series expansion), the bridge output voltage, corresponding to a resistance change of ΔR in the active branch, is $v_s = \dfrac{\Delta R}{4R}v_{ref}$.

Substitute (10) and (11):

$$v_s = \frac{1}{4}\alpha v_{ref}\Delta T \tag{12}$$

Let,

$$v_s = v_n - v_p \tag{13}$$

where, v_n = bridge node potential going toward the −ve lead of the op-amp and v_p is the bridge node potential going to the +ve lead of the op-amp (See Fig. 2).

Now we use the two properties of an op-amp: 1. Current into the op-am from each input lead is zero; 2. The potentials at the two input leads of the op-amp are equal.

Current summation at the inverting input (- lead) node of the op-amp: $\dfrac{v_n - v_p}{R_a} + \dfrac{v_1 - v_p}{R_b} + \dfrac{v_o + v_p - v_p}{R_f} =$ 0 or (from (13)),

$$\frac{v_s}{R_a} + \frac{v_1 - v_p}{R_b} + \frac{v_o}{R_f} = 0 \tag{14}$$

where, v_1 = potential at the junction between C and R_b (see Fig. 2).

$$\rightarrow \qquad v_1 = v_p - \frac{R_b}{R_a}v_s - \frac{R_b}{R_f}v_o \tag{15}$$

Current balance at the junction of C and R_b:

$$C\frac{d(v_n - v_1)}{dt} = \frac{v_1 - v_p}{R_b} \tag{16}$$

Substitute (16) and (15) in (14), to eliminate v_1:

$$\frac{v_s}{R_a} + C\frac{d}{dt}\left[v_n - (v_p - \frac{R_b}{R_a}v_s - \frac{R_b}{R_f}v_o)\right] + \frac{v_o}{R_f} = 0$$

$$\rightarrow(\text{from (13)}) \frac{v_s}{R_a} + C\frac{d}{dt}\left[v_s + \frac{R_b}{R_a}v_s + \frac{R_b}{R_f}v_o\right] + \frac{v_o}{R_f} = 0$$
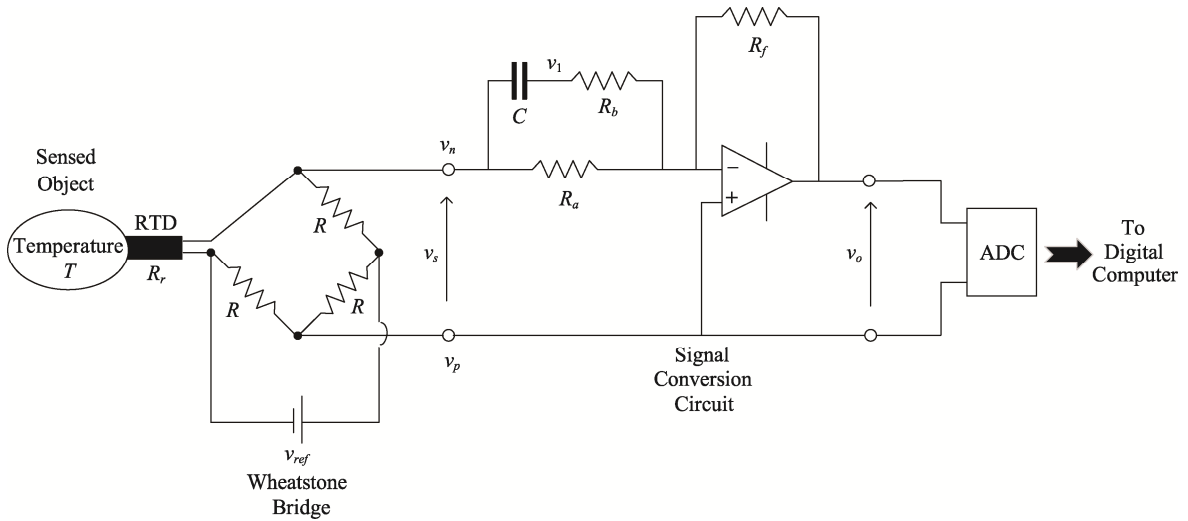

Fig.2   Temperature Monitoring of an Object

$$\rightarrow C\frac{dv_s}{dt}+C\frac{R_b}{R_a}\frac{dv_s}{dt}+\frac{v_s}{R_a}+C\frac{R_b}{R_f}\frac{dv_o}{dt}+\frac{v_o}{R_f}=0$$

$$\rightarrow C\left(1+\frac{R_b}{R_a}\right)\frac{dv_s}{dt}+\frac{v_s}{R_a}=-C\frac{R_b}{R_f}\frac{dv_o}{dt}-\frac{v_o}{R_f}$$

$$\rightarrow CR_f(R_a+R_b)\frac{dv_s}{dt}+R_fv_s=-CR_aR_b\frac{dv_o}{dt}-R_av_o$$

$\rightarrow$ I/O differential equation:

$$R_bC\frac{dv_o}{dt}+v_o=-\frac{R_f}{R_a}\left[(R_a+R_b)C\frac{dv_s}{dt}+v_s\right]\quad(17)$$

In the Laplace domain ($\frac{d}{dt}\Rightarrow s$), we have the circuit transfer function

$$\frac{v_o}{v_s}=G(s)=-\frac{R_f}{R_a}\frac{\left[(R_a+R_b)Cs+1\right]}{(R_bCs+1)}=-k\frac{(\tau_as+1)}{(\tau_bs+1)}$$

where, gain (steady-state value, i.e., at $\omega=0$) $k=\dfrac{R_f}{R_a}$; and time constants $\tau_a=(R_a+R_b)C$ and $\tau_b=R_bC$

As usual, for convenience, we ignore the –ve sign on the transfer function. As we know, the sign in a transfer function (of an op-amp circuit) can be reversed in many ways, and it has no significance in the subsequent analysis.

The corresponding frequency transfer function (obtained by setting $s=j\omega$) is

$$G(j\omega)=k\frac{(\tau_aj\omega+1)}{(\tau_bj\omega+1)}\quad(18)$$

The Bode curves (solid lines) and their asymptotes (broken lines) are shown in Fig. 3. As usual, first the asymptotes are sketched, with appropriate slopes, and then the actual curves are sketched (roughly) based on the asymptotes.

Procedure for obtaining the asymptotes:

At low frequencies: We have $\tau_a\omega\ll1.0$ and $\tau_b\omega\ll1.0$, and they can be neglected wrt 1.0. Hence, $G(j\omega)\rightarrow k$ at low frequencies. This is a "real" value. Its magnitude is

$$k=\frac{R_f}{R_a}\quad(19)$$

This is the steady-state gain.

Its phase angle is 0° (because the transfer function is "real" now).

At intermediate frequencies between $\omega_a=1/\tau_a$ **and** $\omega_b=1/\tau_b$**:** The zero term (i.e., transfer function numerator) $(\tau_aj\omega+1)$ dominates over the pole term (i.e., transfer function denominator) $(\tau_bj\omega+1)$. *Note*: $\tau_a>\tau_b$.

This results in a "phase lead" action, and $G(j\omega)\approx k(\tau_aj\omega+1)$. This provides a magnitude asymptote of +ve slope 20 dB/decade (in log scale), and a phase angle asymptote at 90° (corresponding to the maximum possible lead action, which is the derivative action).

At high frequencies: We have $\tau_a\omega\gg1.0$ and $\tau_b\omega\gg1.0$, and hence 1.0 can be neglected in the pole term and in the zero term. Then, $G(j\omega)\rightarrow$ $k\dfrac{\tau_a}{\tau_b}=\dfrac{R_f(R_a+R_b)}{R_aR_b}=R_f\left(\dfrac{1}{R_b}+\dfrac{1}{R_a}\right)$. This is also a "real" value. Its magnitude is the overall gain now:

$$\text{Gain}=R_f\left(\frac{1}{R_b}+\frac{1}{R_a}\right)\quad(20)$$

Again, the phase angle is 0° (because the transfer function is real).

Note: The break frequencies are $\omega_a=1/\tau_a$ and $\omega_b=1/\tau_b$, which are the points of intersection of the asymptotes.

The important results are the following.

(a) The steady state corresponds to $\omega=0$. From the transfer function (iii), the corresponding gain (the transfer function magnitude) is $k=\dfrac{R_f}{R_a}$, as obtained before.

(b) For high frequencies, $\omega\rightarrow\infty$. From the transfer function (iii), the high-frequency gain (i.e., the transfer function magnitude for $\omega\rightarrow\infty$) is $k\dfrac{\tau_a}{\tau_b}=\dfrac{R_f(R_a+R_b)}{R_aR_b}=R_f\left(\dfrac{1}{R_b}+\dfrac{1}{R_a}\right)$, as obtained be-

fore.

(c) The numerator of $G(j\omega)$ provides a phase lead of $\tan^{-1}\tau_a\omega$. The denominator of $G(j\omega)$ provides a phase lag of $\tan^{-1}\tau_b\omega$. Hence, the overall phase "lead" (in radians) provided by the circuit is $\tan^{-1}\tau_a\omega - \tan^{-1}\tau_b\omega$, where $\tau_a = (R_a + R_b)C$ and $\tau_b = R_b C$.

(d) As indicated before, the break points (in radians/s) of the Bode curve are: $\omega_a = \dfrac{1}{\tau_a}$ and $\omega_b = \dfrac{1}{\tau_b}$.

Benefits of the Circuit:

1. It has two frequency ranges, the low-frequency range and the high frequency range, that provide almost constant signal amplification of gain $\left(\dfrac{R_f}{R_a}\right)$ and $\left(\dfrac{R_f(R_a + R_b)}{R_a R_b}\right)$, respectively, and zero phase change, for the sensor signal.

2. In the intermediate frequency range, it becomes a "lead compensator" providing a phase lead, which has the following benefits of "derivative" or "preview" action: suppressing signal overshoots, speeding up the response, improving the system stability, etc.

3. It provides its very high input impedance to the sensor and its very low output impedance to the ADC (due to the op-amp in the analog circuit), thereby considerably reducing electrical loading.

Now, substitute the given numerical values in $v_s = \dfrac{1}{4}\alpha v_{ref}\Delta T$, for the full scale temperature rise of $\Delta T = 100$ °C. The corresponding sensor output is

$$v_s = \frac{1}{4}\times .008\times 10.0\times 100.0 = 2.0 \text{ V}$$

To realize the best overall sensitivity for the given arrangement, when the sensor generates its full scale voltage (2.0V), the ADC should receive its full-scale input voltage of 6.0 V (which corresponds to $2^8 = 256$ counts). Correspondingly, then, the analog circuit should provide its largest gain. As we have established before, this condition corresponds to the high fre-
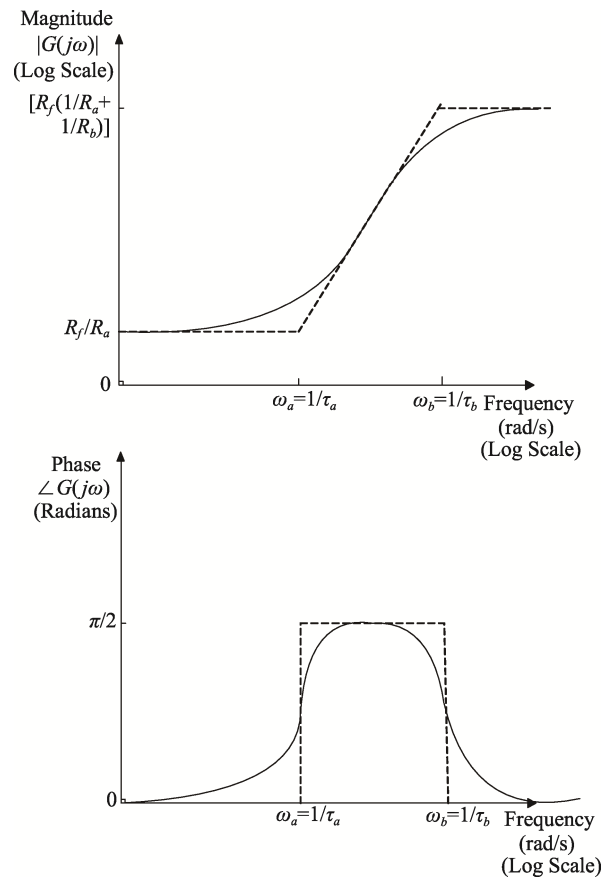
quency range of operation, when the maximum gain (the high-frequency gain) is provided by the circuit.

Hence, the required gain from the circuit = $\dfrac{6.0 \text{ (V)}}{2.0 \text{ (V)}} = 3.0$

The high-frequency gain of the circuit should be equal to this value. Hence,

$$R_f\left(\frac{1}{R_b} + \frac{1}{R_a}\right) = 3.0 = R_f\left(\frac{1}{10.0\times 10^3} + \frac{1}{2.0\times 10^3}\right)$$

$\rightarrow$ $R_f = 5.0\times 10^3\,\Omega = 5.0$ kΩ

Fig.3   Bode Magnitude and Phase Angle Curves of the Circuit

The maximum count of the ADC = $2^8 = 256$ counts. This corresponds to 6.0 V into the ADC. The corresponding temperature rise measured by the sensor is 100.0°C (given). Hence, the overall sensitivity of the device under this condition is $256/100.0$ counts/°C = 2.56 counts/°C.

Note: The sensitivity of the ADC alone is 256 / 6.0 counts/V = 42.7 counts/V

$$\tau_a = (R_a + R_b)C = (10.0 + 2.0) \times 2.0 \times 10^3 \times 10^{-6} = 24.0 \times 10^{-3}\,\text{s}$$

The corresponding break frequency (see Fig. 3),

$$\omega_a = \frac{1}{\tau_a} = \frac{1}{24.0 \times 10^{-3}}\,\text{rad/s} = 41.67\,\text{rad/s} = 6.6\,\text{Hz}$$

$$\tau_b = R_b C = 2.0 \times 2.0 \times 10^3 \times 10^{-6} = 4.0 \times 10^{-3}\,\text{s}$$

The corresponding break frequency (see Fig. 3),

$$\omega_b = \frac{1}{\tau_b} = \frac{1}{4.0 \times 10^{-3}}\,\text{rad/s} = 250.0\,\text{rad/s} = 39.8\,\text{Hz}$$

From Fig. 3 it is clear that there are three possible frequency ranges of operation.

Frequency Range 0.0 to 6.6 Hz (Low frequency range):

In this frequency range, the system (analog circuit in particular) operates in a steady state, with amplification (low-frequency gain) $\frac{R_f}{R_a} = \frac{5.0 \times 10^3}{10.0 \times 10^3} = 0.5$.

The corresponding sensitivity of the overall device is

$$\frac{256\,(\text{counts})}{6.0\,(\text{V})} \times 0.5 \times \frac{2.0\,(\text{V})}{100.0\,(^\circ\text{C})} = 0.43\,\text{counts}/^\circ\text{C}.$$

So, in this range, the sensitivity of the device is relatively poor.

As a rule of thumb (or by Shannon's sampling theorem), a suitable sampling rate in this frequency range should be at least 6.6×2 samples/s → 14 samples/s

Frequency Range 6.6 Hz to 39.8 Hz (Intermediate frequency range):

In this frequency range, the analog circuit functions as a lead compensator. The circuit conditions are dynamic (not steady) as clear from Fig. 3. So, the overall sensitivity will also vary with frequency. However, the device will be more stable (even though dynamic) as the circuit is a lead compensator in this frequency range.

Frequency Range > 39.8 Hz (High frequency range):

In this frequency range as well, the system (ana-log circuit in particular) operates in a steady state. As obtained before, the device will have the best sensitivity then, at 2.56 counts/°C.

As a rule of thumb (or by Shannon's sampling theorem), a suitable sample rate in this frequency range should be at least 39.8×2 samples/s → 80 samples/s. But depending on the high frequency limit of actual operation, the sampling rate should be increased correspondingly (at least to twice the highest frequency of operation).

Let the time constant of the RTD be τ_r. The corresponding break frequency (corner frequency of the Bode curve of the RTD) is $\omega_r = \frac{1}{\tau_r}$.

The frequency range 0 to $\omega_r = \frac{1}{\tau_r}$ rad/s is the nominal flat range of the Bode magnitude curve of the RTD, which is the nominal operating range of frequencies for the RTD. However, close to the break frequency, the magnitude curve is not quite flat (see Fig. 4). So, as a rule of thumb, take the desirable upper operating frequency for the RTD as $\frac{1}{2}\omega_r = \frac{1}{2\tau_r}$. The highest operating frequency of the system is not given in the question. However, for the given numerical values, the lower limit of the upper frequency range of operation has been computed as 39.8 Hz. Now, for example, take the upper frequency limit of operation as 100 Hz. Then we need, $\frac{1}{2\tau_r} = 100.0 \times 2\pi$ rad/s. Or,

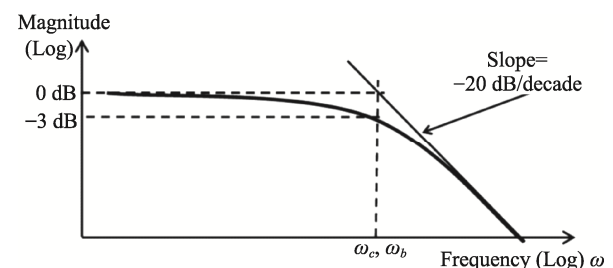$$\tau_r = 0.0008\,\text{s} = 0.8\,\text{ms}.$$

Fig.4   Bode Magnitude Curve of the RTD

4   Error Considerations

Causes for error in a mechatronic system (having interconnected and interacting multiple components) include: Instrument instability, noise and external disturbances (undesirable inputs), poor calibration, system errors (due to inaccurate analytical models, control laws, etc.), parameter changes (e.g., from environmental changes, aging, and wear), unknown nonlinearities, sensor errors, and improper use of the instruments (measurement setup, operating conditions, human error, etc.). These can be in the form of signal errors (at source) and measurement errors. They can depends on calibration, physical hardware, actual operating conditions (power, signal levels, load, speed, environmental factors, etc.), design operating conditions (operating conditions for which the instrument is designed for: normal, steady operating conditions; extreme operating conditions), extreme transient conditions (e.g., emergency start-up and shutdown conditions), instrument setup shortcomings, and other components and systems to which the instrument is connected (e.g., dynamic coupling, loading, or noise from other connected devices).

In this context it is important to know:

(a) How component errors are reflected in the final output—error propagation

(b) Combining component errors—error combination.

Both these depend on the errors in the system components (their variables and parameters), their errors, and how they interact; the measured variables or parameters (of individual components, etc.) that are used to compute (estimate) the required quantity (variable or parameter value); and the relation among components (model). Then, it is important to know:

How component errors propagate within a multicomponent system (Error propagation)

How individual errors in variables/parameters contribute toward overall error (Error combination)

4.1   Analytical Basis for Error Combination

Component contribution to the system output may be expressed as

$$y = f(x_1, x_2, \ldots, x_r) \tag{21}$$

Here, x_i = independent system variable/parameter values whose errors propagate/combine into error in the output y (or required parameter value), represented by increment of y). Take increments, which represent the associated error,

$$\delta y = \frac{\partial f}{\partial x_1} \delta x_1 + \frac{\partial f}{\partial x_2} \delta x_2 + \ldots\ldots + \frac{\partial f}{\partial x_r} \delta x_r \tag{22}$$

The fractional error is given by,

$$\frac{\delta y}{y} = \sum_{i=1}^{r} \left[\frac{x_i}{y} \frac{\partial f}{\partial x_i} \frac{\delta x_i}{x_i} \right] \Rightarrow e_y = \sum_{i=1}^{r} \left[\frac{x_i}{y} \frac{\partial f}{\partial x_i} e_i \right] \tag{23}$$

Here,

$\delta y/y = e_y$ = overall (propagated) error (fractional and nondimensional)

$\delta x_i/x_i = e_i$ = component error (fractional and non-dimensional)

$\dfrac{x_i}{y} \dfrac{\partial f}{\partial x_i}$ = sensitivity of error in x_i on the combined (propagated) error in y (non-dimensional)

From (23) we can express the absolute error as,

$$e_{ABS} = \sum_{i=1}^{r} \left| \frac{x_i}{y} \frac{\partial f}{\partial x_i} \right| e_i \tag{24}$$

This is an upper bound (conservative estimate) for the overall error (*Note*: The individual terms in the sum (23) may be negative)

The SRSS (Square Root of Sum of Squares) error may be expressed as,

$$e_{SRSS} = \left[\sum_{i=1}^{r} \left(\frac{x_i}{y} \frac{\partial f}{\partial x_i} e_i \right)^2 \right]^{1/2} \tag{25}$$

Note: $e_{SRSS} < e_{ABS}$ when two or more nonzero error contributions are present

SRSS is particularly suitable when the component error is represented by the standard deviation of the associated variable/parameter value and when the corresponding error sources are independent.

The degree of importance of component error is measured by the non-dimensional sensitivity: $\dfrac{x_i}{y} \dfrac{\partial f}{\partial x_i}$

These results are useful in: 1. Design of multicomponent systems; 2. Cost effective selection of instru-

mentation, including sensors.

4.2 Case Study

Consider an RTD (a temperature sensor) that has the empirical relation, relating its resistance R (in Ω) and the measured temperature rise ΔT (in °C), given by

$$R_r = R_{r0}(1 + \alpha \Delta T) \qquad (26)$$

where,

R_r = resistance of the RTD, in ohms (Ω), at temperature T (in °K)

T_0 = starting temperature, which is accurately known

$\Delta T = T - T_0$ = temperature rise (in °C)

α = temperature coefficient of RTD resistance (in /°C). It is known very accurately.

Also, consider a thermistor (a temperature sensor) that has the empirical relation, relating its resistance R_t (in Ω) and the measured temperature T (in °K), given by,

$$R_t = R_{t0} \exp\left[\beta\left(\frac{1}{T} - \frac{1}{T_0}\right)\right] \qquad (27)$$

where,

β = characteristic temperature of the thermistor (a positive quantity, in °K). It is known very accurately

T_0 = starting temperature, which is accurately known.

We will determine the relationships between R_{r0} and T_0, and R_{t0} and T_0.

In a typical sensing procedure for temperature, the resistance R of the sensor is measured and (26) or (27), the RTD model or the thermistor model, is used to compute the corresponding temperature T. There is measurement error in R_r and R_t, and model error in R_{r0} and R_{t0}. We will assume that α and β are known accurately. We will determine the expressions (in terms of the indicated model parameters) for the sensitivity of the RTD and the sensitivity of the thermistor (in Ω/°C).

Using the "absolute error" method, we will derive an equation for the combined fractional error e_T in the temperature (estimation) from the RTD, in terms of the

fractional errors e_{R_r} and $e_{R_{r0}}$ of R_r and R_{r0}, respectively. From the result, we will study the effect of a larger T (i.e., larger ΔT) on the fractional error in the determined temperature.

Next, using the "absolute error" method, we will derive an equation for the combined fractional error e_T in the temperature (estimation) from the thermistor, in terms of the fractional errors e_{R_t} and $e_{R_{t0}}$ of R_t and R_{t0}, respectively. From this relation, we will show that a larger T will result in larger fractional error in the determined temperature.

Suppose that for the thermistor,

$R_{t0} = 5000$ Ω at $T_0 = 298$°K (i.e., 25°C) and $\beta = 4200$°K . We will compute the sensitivity (in Ω/°C) of the thermistor in the neighborhood of temperature T_0. Compute the value of the RTD parameter R_{r0} for the RTD to have this same sensitivity, with $\alpha = 0.008$/°C.

Now use the same numerical values as in Part (d). For the RTD, given that $e_{R_r} = \pm 0.01$ and $e_{R_{r0}} = \pm 0.02$, compute the fractional error e_T in the determined (estimated) temperature from the RTD in the neighborhood of temperature T_0. Also, for the thermistor, given that $e_{R_t} = \pm 0.01$ and $e_{R_{t0}} = \pm 0.02$, compute the fractional error e_T in the determined (estimated) temperature from the thermistor in the neighborhood of temperature T_0. From these values we will determine which sensor is more accurate in the temperature measurement, in the given temperature neighborhood.

The characteristic curve of the RTD is sketched in Fig. 5. Consider the given RTD model (26). Set $T = T_0$ (i.e., $\Delta T = 0.0$). Then $R = R_{r0}$. This means that the empirical parameter R_{r0} is the resistance of the RTD at the reference temperature T_0. These key points of RTD are marked in Fig. 5.

The characteristic curve of the thermistor is sketched in Fig. 5. Consider the given thermistor model (27). Set $T = T_o$. Then the exponent becomes zero, and its exponential value is 1. Hence, then $R = R_{t0}$. This means that the empirical parameter R_{t0} is the resistance of the thermistor at the reference

temperature T_0. Next, let $T \to \infty$. Then the exponent becomes $-\dfrac{\beta}{T_0}$. Hence, the resistance at very large values of temperature is $R_{t\infty} = R_{t0} \exp\left[-\dfrac{\beta}{T_0}\right] = \dfrac{R_{t0}}{\exp\left[\dfrac{\beta}{T_0}\right]}$. *Note*: This value is $< R_{t0}$. These key points of thermistor are marked in Fig. 5.

For the RTD,

$$R_r = R_{r0}\left[1 + \alpha(T - T_0)\right] \tag{28}$$

Hence, the RTD sensitivity,

$$\frac{dR_r}{dT} = R_{r0}\alpha \tag{29}$$

N*ote*: The input to sensor is the temperature change, and the corresponding output of the sensor is the resistance change (of course, in practice, that resistance change is converted in a bridge output etc.

For the thermistor, we have (27). Hence, the thermistor sensitivity is,

$$\frac{dR_t}{dT} = R_{t0} \exp\left[\beta\left(\frac{1}{T} - \frac{1}{T_0}\right)\right]\left[-\frac{\beta}{T^2}\right] = -\frac{\beta}{T^2} R_{t0} \exp\left[\beta\left(\frac{1}{T} - \frac{1}{T_0}\right)\right] \tag{30}$$

In the RTD model (28), take the differentials of the individual terms. *Note*: There cannot be an error in the reference temperature T_o itself, because it is a value that one is free to select, and is known to be accurate. Also, since α is very accurate (given), it too cannot have error. Of course, there will be errors in the associated resistance R_{r0}. We get, $\delta R_r = R_{r0}\alpha\delta T + \left[1 + \alpha(T - T_0)\right]\delta R_{r0}$. Divide throughout by R_{r0}.

$\dfrac{\delta R_r}{R_{r0}} = \alpha\delta T + \left[1 + \alpha(T - T_0)\right]\dfrac{\delta R_{r0}}{R_{r0}}$. Since $R \approx R_{r0}$, we have $\dfrac{\delta R_r}{R_{r0}} \approx \dfrac{\delta R_r}{R_r}$ $\to e_{Rr} = \alpha T e_T + [1 + \alpha(T - T_0)]e_{R_{r_0}}$ $\to$ $e_T = \dfrac{1}{\alpha T}\left\{e_{Rr} - \left[1 + \alpha(T - T_0)\right]e_{R_{r_0}}\right\}$.

Or,

$e_T = \dfrac{1}{\alpha T}\left\{e_{Rr} - \left[1 + \alpha\Delta T\right]e_{R_{r_0}}\right\}$. With the absolute method of error combination,

$$e_T = \frac{1}{\alpha T}\left\{e_{Rr} + \left[1 + \alpha\Delta T\right]e_{R_{r_0}}\right\} \tag{31}$$

Note: We use of the "+" sign instead of "−" on the RHS of the error equation since we employ the "absolute" method of error combination (i.e., positive magnitudes are used regardless of the actual algebraic sign). However, each error value is $\pm$. There is a "T" term in both numerator and denominator of the RHS of (31). Hence, its effect (whether increasing or decreasing the RHS) is not immediately clear. We address this issue as follows. We write (31) as $e_T = \dfrac{1}{T}(a + bT)$, where,

$$a = \frac{1}{\alpha}\left\{e_{Rr} + (1 - \alpha T_0)e_{R_{r_0}}\right\} \ \text{and} \ b = e_{R_{r_0}} > 0$$

The sign of a depends on the values of the parameters of the numerator of the expression (Roughly, $a > 0$ if $\alpha T_0 < 2$ and $a < 0$ if $\alpha T_0 > 2$). However, e_T is much smaller than 1.0 and is >0.0 (because it is a "magnitude with an associated $\pm$). See Fig. 6. Whether e_T increases or decreases with T depends on the sign of a (specifically, decreases if $a>0$ and increases if $a<0$). In summary, for an RTD, the effect of a larger T (i.e., larger ΔT) on the error in the determined temperature is not straightforward, and depends on the values of α and T_0.

For a thermistor, write the sensor equation (27) as,

$$\ln R_t - \ln R_{t0} = \beta\left(\frac{1}{T} - \frac{1}{T_0}\right) \ \text{and take the differ-}$$

entials of the individual terms. *Note*: There cannot be an error in the reference temperature T_o itself, because it is a value that one is free to select, and is known to be accurate. Also, since β is very accurate (given), it cannot have error. Of course, there will be errors in the associated resistance R_{t0}.

$$\frac{\delta R_t}{R_t} - \frac{\delta R_{t0}}{R_{t0}} = -\beta\frac{\delta T}{T^2} \quad \to \quad e_R - e_{R_{t_0}} = -\frac{\beta}{T}e_T .$$

With the absolute method of error combination,

$$e_T = \frac{T}{\beta}(e_{R_t} + e_{R_{t0}}) \qquad (32)$$

Note: We use of the "+" sign instead of "−" on the RHS of the error equation since we employ the "absolute" method of error combination (i.e., positive magnitudes are used regardless of the actual algebraic sign). However, each error value is $\pm$. It is clear from (32) that, for a thermistor, a larger T will result in larger fractional error in the determined temperature.
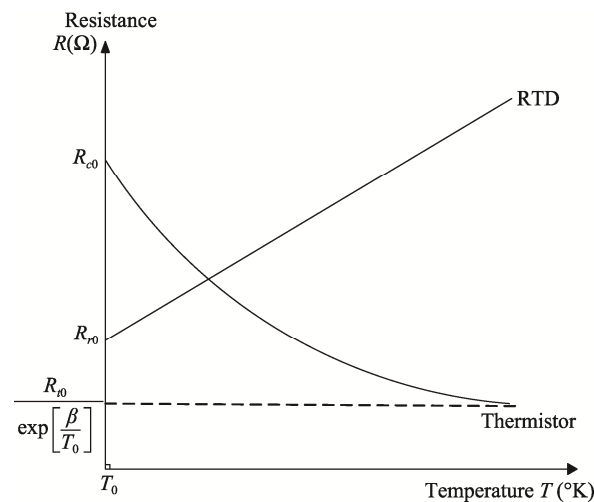
Fig.5   Characteristic Curves of RTD and Thermistor

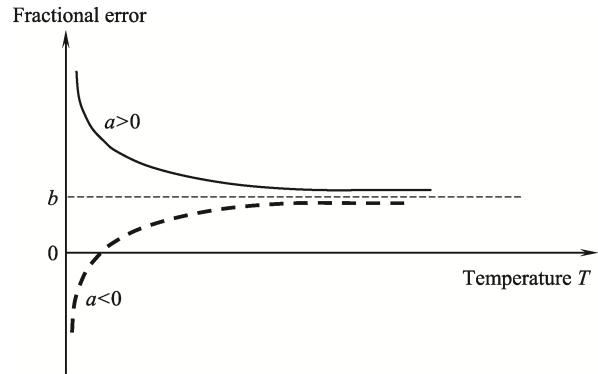For the thermistor, the sensitivity (3) $\approx -\dfrac{\beta}{T^2}R_{t0}$ near T_0 (i.e., $T \approx T_0$). With,

$R_{t0} = 5000\ \Omega$ at $T_0 = 298°K$ (i.e., 25°C)   and $\beta = 4200°K$,

$$\frac{dR_t}{dT} \approx -\frac{\beta}{T^2}R_{t0} = -\frac{4200.0}{298.0^2} \times 5000.0 = -236.5\ \Omega/°K.$$

For the RTD to have the same sensitivity (with α=0.008/°C),   we need $\dfrac{dR_r}{dT} = R_{r0}\alpha = R_{r0} \times 0.008 = 236.5$.

Note: The sign of a sensitivity value is immaterial).

$$\rightarrow \quad R_{r0} = \frac{236.5}{0.008} = 30000.0\ \Omega$$

Fig.6   The Effect of the Sign of *a*

For the RTD, the error relation (31) $\approx \dfrac{1}{\alpha T}(e_{Rr} + e_{R_{r0}})$ in the neighborhood of $T \approx T_0$.

Now substitute the given numerical values for RTD:

$$e_T = \frac{1}{0.008 \times 298.0}(0.01 + 0.02) = 0.0126 \approx \pm 0.013$$

For thermistor, substitute the given numerical values in (32): $e_T = \dfrac{400}{4200}(0.01 + 0.02) = 0.003$

It follows that the temperature estimate from the RTD is much less accurate than that from the thermistor.

5   Conclusions

The focus of the present paper was the optimal matching of sensors with other hardware in the system. The present paper explored the fact that sensor matching was based on such concepts as the operating frequency range (operating bandwidth), speed of response (and the corresponding rate of data sampling in digital conversion), the device sensitivity (or data amplification), and the effect of component accuracy on the overall accuracy of the system. Also, the present paper presented suitable approaches for sensor matching through these criteria. The relevant procedures were illustrated using case studies. It was concluded that optimal matching of the system components is implicit in the proper definition of a mechatronic system.

Acknowledgment

References

[1] De Silva, C.W. (2018). *MODELING OF DYNAMIC SYSTEMS—With Engineering Applications*, Taylor & Francis/CRC Press, Boca Raton, FL.

[2] Joshi, S. and Boyd, S., "Sensor Selection via Convex Optimization," *IEEE Transactions on Signal Processing*, Vol. 57, No. 2, pp. 451-462, 2009.

[3] Simidjievski, N., Todorovski, L., and Dzeroski, S. (2015). "Predicting long-term population dynamics with bagging and boosting of process-based models," *Expert Systems with Applications*, Vol. 42, No. 22, pp. 8484–8496.

[4] Iskander, J., Hossny, M., Nahavand, S., and del Porto, L. (2018). "An ocular biomechanic model for dynamic simulation of different eye movements," *Journal of Biomechanics*, Vol. 71, pp. 209-216.

[5] Lang, H., Wang, Y., and de Silva, C.W. (2017). "Semi-empirical Modeling and Parameter Analysis for the Development of a High Speed Resistance-welding Process," *International Journal of Modelling and Simulation*, pp. 1-9.

[6] Lee, T.H., Liang, W., de Silva, C.W., and Tan, K.K., *Force and Position Control of Mechatronic Systems—Design and Applications in Medical Devices*, Springer, Gewerbestrasse, Switzerland, 2020.

[7] De Silva, C.W., *SENSOR SYSTEMS—Fundamentals and Applications*, Taylor & Francis/CRC Press, Boca Raton, FL, 2016.

[8] De Silva, C.W., SENSORS AND *ACTUATORS— Engineering System Instrumentation*, 2nd Edition, Taylor & Francis/CRC Press, Boca Raton, FL, 2016.

Author Biographies

Clarence W. DE SILVA, received the Ph.D. degrees from the Massachusetts Institute of Technology, Cambridge, MA, USA, in 1978, and from the University of Cambridge, Cambridge, U.K., in 1998, the honorary D.Eng. degree from the University of Waterloo, Waterloo, ON, Canada, in 2008, and the Higher Doctorate, Sc.D., from the University of Cambridge in 2020. He is a Professor of mechanical engineering at The University of British Columbia, Vancouver, BC, Canada. He is a fellow of: IEEE, ASME, Canadian Academy of Engineering, and Royal Society of Canada. His appointments include the Tier 1 Canada Research Chair in Mechatronics and Industrial Automation, Professorial Fellow, Peter Wall Scholar, Mobil Endowed Chair Professor, and NSERCBC Packers Chair in Industrial Automation. His recent books, published by Taylor & Francis/CRC Press, include *Modeling of Dynamic Systems–With Engineering Applications* (2018), *Sensor Systems* (2017), *Sensors and Actuators–Engineering System Instrumentation*, 2nd Edition (2016), *Mechanics of Materials* (2014), *Mechatronics–A Foundation Course* (2010), *Modeling and Control of Engineering Systems* (2009), and *VIBRATION–Fundamentals and Practice*, 2nd Edition (2007); and by Addison Wesley, *Soft Computing and Intelligent Systems Design– Theory, Tools, and Applications* (with F. Karray, 2004).

Email: desilva@mech.ubc.ca